

Can we use Next-Generation Gravitational Wave Detectors for Precision Measurements of Shapiro Delay?

Andrew G. Sullivan,¹ Doğa Veske,¹ Zsuzsa Márka,² Imre Bartos,³ Stefan Ballmer,⁴ Peter Shawhan,⁵ and Szabolcs Márka¹

¹*Department of Physics, Columbia University in the City of New York, New York, NY 10027, USA*

²*Columbia Astrophysics Laboratory, Columbia University in the City of New York, New York, NY 10027, USA*

³*Department of Physics, University of Florida, Gainesville, FL 32611-8440, USA*

⁴*Department of Physics, Syracuse University, Syracuse, NY 13210, USA*

⁵*Department of Physics, University of Maryland, College Park, MD 20742, USA*

Shapiro time delay is one of the fundamental tests of general relativity. To date all measurements of time delay have been conducted on astronomical scales. It was asserted in 2010 that gravitational wave detectors on Earth could be used to measure Shapiro delay on a terrestrial scale via massive rotating systems. Building on that work, we consider how measurements of Shapiro delay can be made using next-generation gravitational wave detectors. We perform an analysis for measuring Shapiro delay with the next-generation gravitational wave detector Cosmic Explorer to determine how precisely the effect can be measured. Using a rotating mass unit design, we find that Cosmic Explorer can measure the Shapiro delay signal with an amplitude signal to noise ratio (SNR) up to ~ 37 in 1 year of integration time. By measuring Shapiro delay with this technique, Cosmic Explorer will allow for terrestrial measurements of γ in the parameterized post-Newtonian formalism of gravity with precision of $< 1\%$.

I. INTRODUCTION

The general theory of relativity suggests a number of observable properties as a consequence of the equivalence principle and spacetime curvature[1]. Improved tests for general relativity continue to be sought in physics to increase the measurement precision and repertoire for testing the theory[2].

One of the long-known tests of these properties lies in measuring the time delay of light as it passes close to massive objects, as first described by Irwin Shapiro in 1964[3]. Shapiro proposed using a radar pulse directed at a planet near the Sun and measuring the delay in the travel time to and from the planet as a result of the presence of the Sun. The one-way time delay for this experiment as predicted by general relativity is given by

$$\delta t = \frac{2GM_{\odot}}{c^3} \ln\left(\frac{4r_1 r_2}{d^2}\right) \quad (1)$$

where G is Newton's gravitational constant, M_{\odot} is the mass of the Sun, c is the speed of light, r_1 and r_2 are the orbital radii of the Earth and the target planet, respectively, and d is the closest distance the light pulse approaches to the center of the Sun. In Shapiro's original formulation there are a number of practical uncertainties in obtaining an exact answer due to initial conditions such as the planetary speeds and locations[4]. For planets in the solar system, however, the time delay is substantial, on the order of 10^{-4} seconds[3].

In the weak field limit, alternative gravity theories can be characterized by the parameterized post-Newtonian (PPN) formalism as deviations from Newtonian gravity [1]. The γ parameter in the PPN formalism, which is related to spacetime curvature produced by a unit mass, can be determined through Shapiro delay measurements.

The generalized formulation for Shapiro time delay in the PPN formalism for any metric theory is given by

$$\delta t = (1 + \gamma) \frac{GM}{c^3} \ln\left(\frac{4r_1 r_2}{d^2}\right) \quad (2)$$

In general relativity, specifically, $\gamma = 1$. A number of experiments and observations have placed limits on the value of γ including observations of planetary echos[5], the Viking relativity experiment[6], measurements of Shapiro delay from quasars due to the presence of Jupiter[7, 8], lunar laser ranging experiments[9], and observations of Mercury's perihelion orbit[10]. The Cassini spacecraft has made the most precise measurement of γ to date, with $(1 - \gamma) = (2.1 \pm 2.3) \times 10^{-5}$, which is in agreement with the predictions of general relativity[11].

All measurements of Shapiro time delay and γ to date have been made on astronomical scales. In 2010, Ballmer et al. proposed a method for measuring Shapiro time delay on a terrestrial scale using an Advanced LIGO (aLIGO)[12] gravitational wave (GW) detector, which could be accomplished by installing a rotating mass unit (RMU) to modulate the gravitational potential along one arm[13]. By building up a periodic change in the curvature of spacetime, delays on the order of 10^{-32} seconds produced by an RMU with 10^4 kg masses were shown to be measurable with an amplitude SNR of ~ 8.7 over an integration time of 1 year.

In 2015, aLIGO began its first observing run [14–16] and currently several future interferometric GW detectors are proposed for 2030-2050 [17–24]. Proposed detectors in the design stage include Cosmic Explorer (CE)[22, 23], the Einstein Telescope (ET)[20, 21], and space based detector LISA[24]. New detectors with substantially better sensitivity will improve the prospect of measuring GW signals and gravitational effects including

Shapiro delay[25] with greater precision.

In this paper, we revisit the previous work on measuring Shapiro delay with RMUs and laser interferometers[13, 26, 27] and investigate the possible improvements of the next-generation gravitational wave detector CE[22, 23]. In Section II, we present the principles behind interferometric gravitational wave detectors and their sensitivities, specifically that of CE. In Section III, we explain the suggested RMU and summarize our choice of rotor geometries. In Section IV, we detail the expected time delay signal from the RMU and compare the signal to the sensitivity of CE. In Section V, we discuss our results and the precision of the measurements we expect to make with this experiment. Finally in Section VI, we consider the implications of Shapiro delay measurements with CE within the context of making higher precision terrestrial measurements of general relativity and conclude.

II. LONG-ARM INTERFEROMETRIC MEASUREMENT PRINCIPLES

Long-arm interferometers operate by making measurements of differences in the length of the interferometer laser arms, making them ideal for measuring GWs, which change the spatial distances during propagation in the weak field limit. GW observation functions via measuring the differential change in the lengths of the arms of a Michelson-type interferometer as a result of a passing GW[28]. Figure 1 depicts the basic design concept of a laser interferometer for GW detection, including the location of the proposed RMU to be discussed in Section III. Laser interferometers serve to achieve sensitivities capable of detecting GWs on Earth with dimensionless strains on the order of 10^{-21} and smaller[28].

Interferometric GW detector technology has continually improved in sensitivity over the last 15 years, through observing runs in a variety of GW detectors including first generation detectors TAMA[29], LIGO[30], Virgo[31], and GEO600[32], and second generation detectors aLIGO[12] and Advanced Virgo (AdVirgo)[33]. A new detector KAGRA[34, 35] has begun operation in 2020 and LIGO-India[36] is expected to be operating in the near future. aLIGO began operation in 2015, demonstrating substantial improvements in noise floor and frequency reach over initial LIGO [12, 30] due to improved measurement techniques. Shortly into its first observing run, the aLIGO gravitational wave detectors proved sensitive enough to detect the first gravitational wave transient ever recorded, from the inspiral and merger of two black holes[37].

CE is the next generation successor to aLIGO in the search for gravitational waves, with much improved sensitivity over aLIGO[22, 23]. CE utilizes a similar Michelson interferometer design shown in Figure 1, including Fabry-Perot cavities and signal recycling mechanisms that increase sensitivity. CE will have arm cavities that are

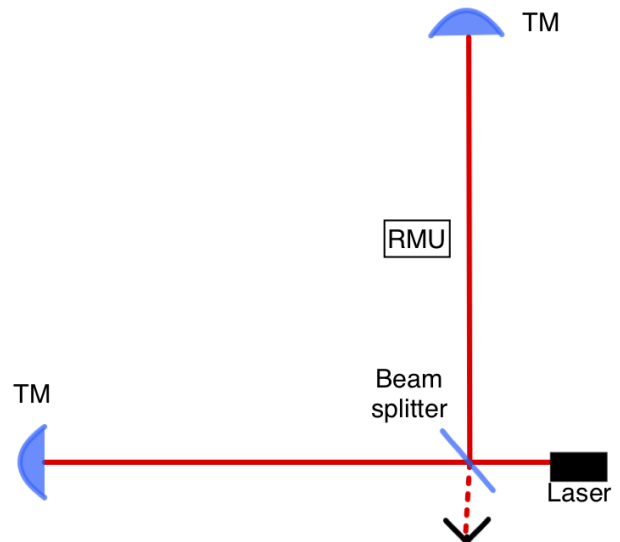


FIG. 1. A diagram of a simplified Michelson interferometer design with test masses (TM) for GW detection, including the location of the proposed RMU in the center of one of the interferometer arms.

40 km in length, a factor of 10 greater than the length of aLIGO's arm cavities at 4 km. In addition to cavity length, CE is expected to employ a number of techniques to reduce noise, including increased mirror reflectivity, increased laser power, and increased test mass[22, 23]. At the low frequency limits, CE will likely be limited by Newtonian gravity gradient and seismic noise[22], while exhibiting greater sensitivity in that range than aLIGO[22]. Figure 2 shows the sensitivity curves for CE, including the sensitivity curve of aLIGO for reference. CE will develop in two stages: CE1 (2030s) and CE2 (2040s), where CE2 will be its design sensitivity[23]. For this study we adopt the sensitivity curve of CE2.

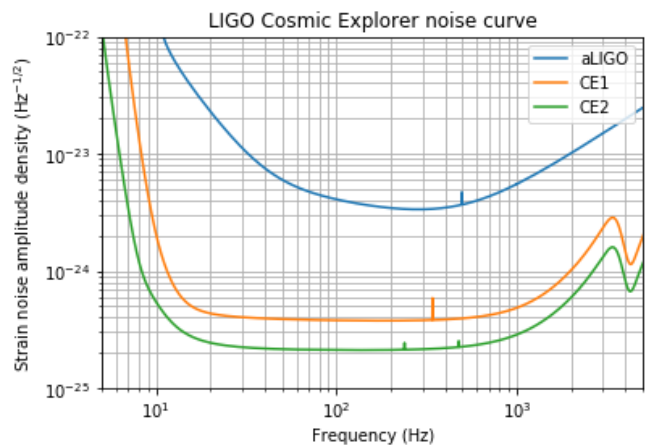


FIG. 2. The proposed one-sided strain noise amplitude density curve for both stages of the CE GW observatory[22, 23], with CE1 in orange and CE2 in green. The sensitivity curve for aLIGO[12] at design sensitivity is included in blue.

III. ROTATING MASS UNIT

Interferometric GW measurement is sensitive to time-varying signals. Therefore, in order for the Shapiro time delay to be measured, the delay must be modulated[13]. A RMU provides a way to modulate the Shapiro delay because the rotation allows for a periodic change in the mass density that produces a phase-coherent signal in the interferometer data stream.

The proposed RMU would operate as follows: a bar structure suspended by its middle with masses concentrated at the ends of the bar would be placed alongside the center of one of the GW detector arms and rotate in the plane perpendicular to the laser beam, as described in [13]. As the assembly rotates, the curvature of space-time through which the laser beam passes changes due to variation in the distance to the masses, thus producing Shapiro delay. To improve precision, an array of multiple RMUs symmetrically arranged alongside the center of one of the GW detector arms may be used. The RMU's rotation would be constantly monitored, ensuring that the data analysis of the Shapiro delay can be done with excellent phase-coherence and precision over long periods of time.

In the Ballmer et al. analysis [13], a symmetric RMU with end masses of 1.5×10^4 kg each 1.5 meters from the axis of rotation was used. In order for the primary harmonic to be in a sensitive frequency range, Ballmer et al. chose the spin frequency of the RMU to be 25 Hz. Those parameters required the system to sustain 6×10^8 N of centripetal force. To achieve this, the proposed structure was made up of steel weight test masses supported by an arm structure wrapped in a carbon fiber frame. Figure 3 shows a sketch of Ballmer et al.'s RMU design.

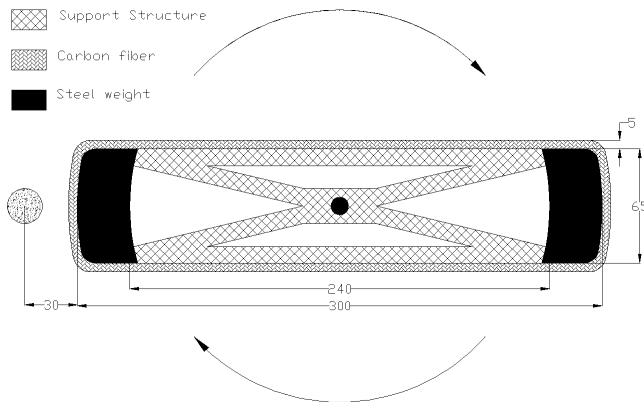


FIG. 3. A sketch of the RMU proposed by Ballmer et al. [13]. Each dimension is measured in centimeters. The circle to the left of the rotating mass represents the interferometer laser beam, placed 30 centimeters from the closest point of the mass. We adopt the same design and structure, but vary the steel mass size to either reduce the expense or maximize the scientific output of such a device. Figure taken from Ballmer et al. Figure 3 [13].

We consider whether a symmetric RMU (i.e. one where the center of mass is located at the center of the bar) is the optimal geometry for measuring the Shapiro delay. The time delay is proportional to a line integral of the Newtonian potential U . The Newtonian potential behaves $\propto \frac{M}{r}$, where M is the mass generating the gravitational field and r is the distance from the mass to the point of interest. For an asymmetric rotor system, the ratio of arm lengths of the rotor would need to be proportional to the inverse ratio of the end masses to maintain a stable axis of rotation (i.e. the smaller mass's minimum distance to the interferometer laser beam is closer than the larger mass's minimum distance).

With the constant constraints of minimum distance to beam, total mass, and total length of the rotor; when compared with the symmetric masses, the maximal contribution from the smaller mass reduces by the factor of the mass ratio since its minimum distance to beam doesn't change. However the maximal contribution from the large mass doesn't increase by the same factor since its minimum distance will be farther. Hence we expect the symmetric design to produce the highest SNR, so we adopt the symmetric geometry like the previous rotating mass system [13].

For our analysis, we propose three possible RMU models using the symmetric geometry described above: an advanced science model, the Ballmer et al. model, and a cost conscious model. We label these three models A, B, and C for convenience. All three models are 3.0 meters in length[13]. The distance of closest approach to the laser beam remains at 30 cm as depicted by Figure 3. We design model A to have end masses of 2.5×10^4 kg and rotate at a frequency of a 25 Hz to most effectively induce detection. To account for the greater steel mass in model A, we propose extending the width of the rotor in the direction parallel to the laser beam to satisfy size constraints. Model B is the exact one described above with 1.5×10^4 kg steel weight end masses, rotating at a frequency of 25 Hz. Model C possesses end masses of 6500 kg and rotates at a lower frequency at 15 Hz, requiring substantially less energy to be stored in the heavy rotating masses, and therefore decreasing material strength and cost requirements. A lower rotational frequency and mass better ensure the safety of operation. Additionally, the relative flatness of the CE noise curve from 20 Hz to about 500 Hz allows for a signal to be measured whose primary harmonic is below 50 Hz.

One constraint to consider in calculating the Shapiro delay is the gravitational coupling attraction between the RMU and the test masses at the end of the laser arm. This acceleration, however, behaves $\propto L^{-6}$, where L is the length of the the interferometer arm cavity. Solving for the position of the interferometer test mass as a function of time, we obtain the amplitude of oscillation for each of the three spatial degrees of freedom. The amplitude of oscillation in the axis along the laser pathway dz

is as follows:

$$dz = \frac{6\sqrt{8}GMl^2(d+l)^2}{L^6(\omega_r^2 - 4\omega^2)} \quad (3)$$

where M is the RMU end mass, d is the closest distance the RMU end mass approaches to the interferometer laser beam, l is half the length of the RMU, ω_r is the angular resonance frequency of the test mass, and ω is the angular frequency of the RMU. The frequencies chosen for all 3 models exceed the greatest resonance frequency for aLIGO, making the $(\omega_r^2 - 4\omega^2)^{-1}$ factor no greater than order ~ 1 , since the resonance frequencies for CE will be even lower. The dz coupling can be neglected for CE, as L is 40,000 m, making the effect on the order of a Planck length. In the directions perpendicular to the laser path (i.e. dx and dy), the coupling behaves $\propto L^{-5}$; however, this coupling has a negligible effect on the motion of the test mass in the direction of the laser arm.

IV. SIGNAL ANALYSIS

The time delay of a light signal passing near a massive object is given by

$$\delta t = \int (1 + \gamma)U ds \quad (4)$$

in the weak field limit^[1] where the integral is over the signal path and U is the Newtonian potential scaled with the reciprocal of the cube of speed of light

$$U = \sum_{i=1}^N \frac{GM_i}{c^3 r_i} \quad (5)$$

for N masses, where c is the speed of light and r_i is the distance to each mass M_i . For this arrangement of one RMU, it corresponds to the distance from the interferometer's laser beam to the masses at the ends of the rotor, and $N = 2$. To produce a signal with a larger amplitude one can determine the potential for an arrangement of multiple RMUs. For this principle study we calculate the signals produced by one RMU.

To evaluate the time delay, we simplify the geometry of each RMU for our calculations, assuming the end masses to be point masses and the support systems holding them up to have negligible mass for this proof of concept demonstration (Ballmer et al. do not make this assumption in their paper, leading to a difference in SNR of about 10% from what we report here). As previously mentioned, we require all RMU models to be 3.0 meters in length and the minimum distance between the RMU and the laser beam to be 30 centimeters. By evaluating the integral in Equation (4) for each of our three models, we obtain the Shapiro time delay as a function of

time. Time delays for our three models are shown in Figure 4, with variations on the order of 10^{-31} seconds for models A and B, and 10^{-32} seconds for model C. This corresponds to an optical distance change on the order of 10^{-23} meters for all three models, displacements that CE will have the capability to measure.

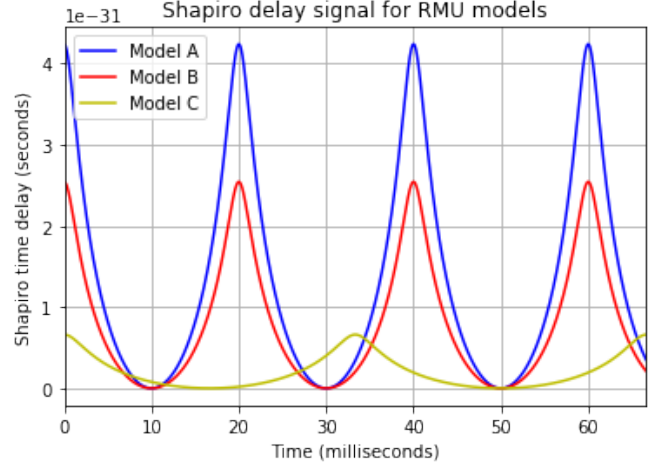


FIG. 4. The time delay as a function of time for all models over 67 milliseconds, the period of rotation for model C. Models A and B rotate at 25 Hz and model C rotates at 15 Hz.

Having calculated the Shapiro delay signal for each RMU model using Equation (4), we calculate a total SNR over 1 year for the three models with the proposed noise curve for CE by using matched filtering and assuming our signals are periodic, so that their Fourier transforms have impulses. We also find the SNRs for the individual Fourier components of each signal. We quote 1 year of integration time results as a basis since SNR grows proportionally to the square root of time. (See [38] for note on long data taking). Our results are listed in Table I.

As Table I indicates, we find that the total SNR for 1 year of integration time to be 37 for model A. Additionally, model B yields an SNR of 22, and model C yields an SNR of 9.1. For model A, the fundamental frequency at 50 Hz is observable with an SNR of 34, while the second and third harmonics have SNRs of 12 and 5.5 (including both the positive and negative frequency components), respectively, over 1 year of integration time. For the signal produced by model B, the SNR for the fundamental frequency is 20; second and third harmonics have SNRs of 7.1 and 3.3 respectively for 1 year of integration time. Model C generates a signal whose fundamental frequency will be observable with an SNR of 8.4, and second harmonic with an SNR of 3.1 in 1 year of integration time.

Model	A	B	C
End Mass (kg)	2.5×10^4	1.5×10^4	6.5×10^3
Rotational Frequency (Hz)	25	25	15
Total SNR	37	22	9.1
Primary Harmonic SNR	34	20	8.4
Secondary Harmonic SNR	12	7.1	3.1

TABLE I. The 1 year total SNR and SNRs for the primary and secondary harmonic for each of the three models. We include the end mass and rotational frequency of each RMU model for referential convenience.

We show the Fourier series coefficients of each model's signal and compare them to the CE sensitivity curve for 1 year of integration time in Figure 5. Note that model C has Fourier series coefficients at different frequencies than the other two models because it oscillates at 15 Hz rather than 25 Hz, making the Fourier components multiples of 30 Hz rather than 50 Hz (the factor of 2 comes from the mass symmetry).

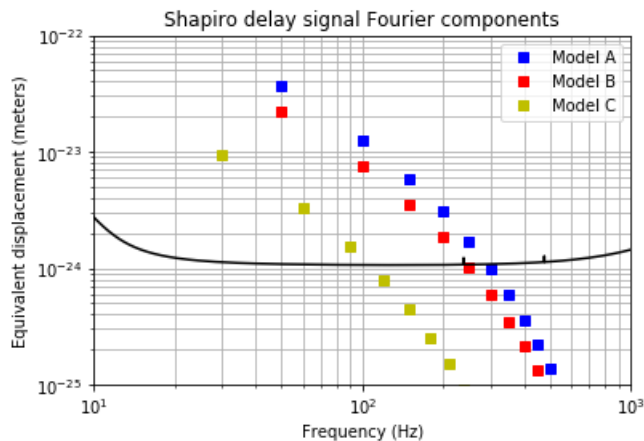


FIG. 5. The Fourier series coefficients of the Shapiro delay signal converted to the equivalent light path displacement as a result of the delay produced by each of the three RMU models. The black solid line is the noise amplitude curve for CE2 at design sensitivity for 1 year of integration time.

V. DISCUSSION

The prior analysis showed that aLIGO has the capability to probe Shapiro delay on a terrestrial level; however, a rotor with 1.5×10^4 kg end masses would only yield an SNR of 9.5 in 1 year of integration time (making the point mass assumption). Observing the Shapiro delay with that SNR would allow for a measurement of γ with $\sim \pm 25\%$ precision for one standard deviation[13].

Results for our three RMU models demonstrate the new experimental gravity test that can be feasibly achieved with CE. Our model A with 2.5×10^4 kg end masses produces a Shapiro delay with a total SNR over

~ 37 in 1 year, substantially better than the scenario considered by Ballmer et al. By directly comparing the signal results produced by the model B to the results from Ballmer et al., we find that the CE interferometer yields vastly superior measurement capabilities to aLIGO, as CE will measure a total SNR of ~ 22 rather than ~ 9.5 in 1 year of integration time, ~ 2.3 times larger.

Model C possesses the most conservatively sized masses: less than half of that of the rotor system 1.5×10^4 used in the Ballmer et al. calculation, and still produces a signal with an SNR of 9.1. This would achieve a similar level of precision expected by Ballmer et al. in 1 year of integration time, but, because of CE's advanced sensitivity, will cost less material and energy to operate and improve measurement precision as the integration time increases. Additionally, our results for the low cost model demonstrate that the rotor can operate at a lower frequency and still produce appreciable results. Because of CE's flat noise curve from 30 Hz onward, utilizing an RMU that rotates at a lower frequency would be feasible.

Assuming Gaussian distributed noise, the delay measurements are expected to yield a Gaussian distributed measurement of $(1+\gamma)$ with the mean squared to variance ratio being equal to the square of the expected amplitude SNR. Thus we can obtain an expected precision for our measurements with the determined SNRs. With model B, the model used in Ballmer et al., CE can obtain a measurement of the Shapiro delay with up to $\pm \sim 4.5\%$ precision and γ with up to $\pm \sim 9\%$ precision. Using our advanced science model A, we expect to achieve measurements of γ with a precision up to $\pm 5\%$ with just 1 year of observation. Precision also increases with time[38], so over longer times and with the use of multiple synchronized RMUs, this technique can achieve sub-percent precision measurements. An arrangement of three synchronized model A RMUs can measure γ with precision under $\pm 1\%$ in 10 years.

VI. CONCLUSION

We presented an analysis that details the use an RMU with the next-generation GW detector CE to measure Shapiro delay. Despite all prior Shapiro delay measurements being space based experiments, we show that RMU models are capable of generating a substantial Shapiro

delay signals measurable on Earth using CE. As detailed in our discussion, our RMU produces a signal with an appreciable SNR in 1 year of observation with CE. This corresponds to the most precise proposed Earth-based measurement scheme of γ to date with a noticeable increase in the measurement precision achievable with aLIGO, as CE can measure γ with up to $\pm \sim 5\%$ precision in just 1 year with the installation of one RMU.

This technique has its limitations, as it does not yet approach the level of precision achieved by longer range, space-based experiments such as that of the Cassini spacecraft, which achieved a precision of $\sim 0.005\%$ in 6 years of observation[11]. In 6 years of observation time with CE and one RMU, this technique would yield a precision of $\pm 2\%$. An array of synchronized RMUs, however, would increase the precision, achieving sub-percent measurements within a decade. Applying this analysis to ET will further this study. Nevertheless, CE promises to

be capable of probing exciting gravity science including precise measurements of Shapiro delay and γ on Earth.

ACKNOWLEDGMENTS

The authors thank Columbia University in the City of New York, University of Florida, Syracuse University, and University of Maryland for their generous support. The Columbia Experimental Gravity group is grateful for the generous support of the National Science Foundation under grant PHY-1708028. AS is grateful for the support of the Columbia College Science Research Fellows program. DV is grateful to the Ph.D. grant of the Fulbright foreign student program and the Jacob Shaham Fellowship. PS is grateful for the support of the National Science Foundation through grant PHY-1710286. SB is grateful for the support of the National Science Foundation through grant PHY-1836702.

-
- [1] C. M. Will, *Theory and Experiment in Gravitational Physics* (Cambridge University Press, 1993).
 - [2] J. Schiffrin and R. Wald, in *APS April Meeting Abstracts*, Vol. 2012 (2012) p. X8.002.
 - [3] I. I. Shapiro, *Phys. Rev. Lett.* **13**, 789 (1964).
 - [4] I. I. Shapiro, *Physical Review* **141**, 1219 (1966).
 - [5] C. M. Will, *Science* **250**, 770 (1990).
 - [6] R. D. Reasenberg, I. I. Shapiro, P. E. MacNeil, R. B. Goldstein, J. C. Breidenthal, J. P. Brenkle, D. L. Cain, T. M. Kaufman, T. A. Komarek, and A. I. Zygielbaum, *ApJ* **234**, L219 (1979).
 - [7] S. M. Kopeikin, *Physics Letters A* **312**, 147 (2003), [arXiv:gr-qc/0212121 \[gr-qc\]](#).
 - [8] E. B. Fomalont and S. M. Kopeikin, *ApJ* **598**, 704 (2003), [arXiv:astro-ph/0302294 \[astro-ph\]](#).
 - [9] J. Battat, N. Colmenares, R. Davis, L. H. Ruixue, J. Murphy, Thomas W., and Apollo Collaboration, in *APS April Meeting Abstracts*, APS Meeting Abstracts, Vol. 2017 (2017) p. B3.001.
 - [10] L. Iorio, in *36th COSPAR Scientific Assembly*, Vol. 36 (2006) p. 182.
 - [11] B. Bertotti, L. Iess, and P. Tortora, *Nature* **425**, 374 (2003).
 - [12] LIGO Scientific Collaboration, J. Aasi, B. P. Abbott, R. Abbott, T. Abbott, M. R. Abernathy, K. Ackley, C. Adams, T. Adams, and P. Addesso, *Classical and Quantum Gravity* **32**, 074001 (2015), [arXiv:1411.4547 \[gr-qc\]](#).
 - [13] S. Ballmer, S. Márka, and P. Shawhan, *Classical and Quantum Gravity* **27**, 185018 (2010), [arXiv:0905.0687 \[gr-qc\]](#).
 - [14] G. M. Harry and LIGO Scientific Collaboration, *Classical and Quantum Gravity* **27**, 084006 (2010).
 - [15] C. J. Moore, R. H. Cole, and C. P. L. Berry, *Classical and Quantum Gravity* **32**, 015014 (2015), [arXiv:1408.0740 \[gr-qc\]](#).
 - [16] D. V. Martynov, E. D. Hall, B. P. Abbott, R. Abbott, T. D. Abbott, C. Adams, R. X. Adhikari, R. A. Anderson, S. B. Anderson, and K. Arai, *Phys. Rev. D* **93**, 112004 (2016), [arXiv:1604.00439 \[astro-ph.IM\]](#).
 - [17] S. Hild *et al.*, *Classical and Quantum Gravity* **28**, 094013 (2011).
 - [18] C. Van Den Broeck, in *Journal of Physics Conference Series*, Journal of Physics Conference Series, Vol. 484 (2014) p. 012008, [arXiv:1303.7393 \[gr-qc\]](#).
 - [19] S. Hild, S. Chelkowski, A. Freise, J. Franc, N. Morgado, R. Flaminio, and R. DeSalvo, *Classical and Quantum Gravity* **27**, 015003 (2009).
 - [20] M. Punturo, M. Abernathy, F. Acernese, B. Allen, N. Andersson, K. Arun, F. Barone, B. Barr, M. Barsuglia, M. Beker, *et al.*, *Classical and Quantum Gravity* **27**, 194002 (2010).
 - [21] M. Maggiore, C. Van Den Broeck, N. Bartolo, E. Belgacem, D. Bertacca, M. A. Bizouard, M. Branchesi, S. Clesse, S. Foffa, J. García-Bellido, *et al.*, *J. Cosmology Astropart. Phys.* **2020**, 050 (2020), [arXiv:1912.02622 \[astro-ph.CO\]](#).
 - [22] B. P. Abbott, R. Abbott, T. D. Abbott, M. R. Abernathy, K. Ackley, C. Adams, P. Addesso, R. X. Adhikari, V. B. Adya, and C. Affeldt, *Classical and Quantum Gravity* **34**, 044001 (2017), [arXiv:1607.08697 \[astro-ph.IM\]](#).
 - [23] D. Reitze, R. X. Adhikari, S. Ballmer, B. Barish, L. Barsotti, G. Billingsley, D. A. Brown, Y. Chen, D. Coyne, and R. o. Eisenstein, in *BAAS*, Vol. 51 (2019) p. 35, [arXiv:1907.04833 \[astro-ph.IM\]](#).
 - [24] P. Amaro-Seoane, H. Audley, S. Babak, J. Baker, E. Barausse, P. Bender, E. Berti, P. Binetruy, M. Born, D. Bortoluzzi, J. Camp, C. Caprini, V. Cardoso, *et al.*, *arXiv e-prints*, [arXiv:1702.00786](#) (2017), [arXiv:1702.00786 \[astro-ph.IM\]](#).
 - [25] B. Chauvineau, S. Pireaux, and T. Regimbau, *Classical and Quantum Gravity* **24**, 3005 (2007), [arXiv:0908.2043 \[gr-qc\]](#).
 - [26] L. Matone, P. Raffai, S. Marka, R. Grossman, P. Kalmus, Z. Marka, J. Rollins, and V. Sannibale, *arXiv e-prints*, [gr-qc/0701134](#) (2007), [arXiv:gr-qc/0701134 \[gr-qc\]](#).

- [27] P. Raffai, G. Szeifert, L. Matone, Y. Aso, I. Bartos, Z. Márka, F. Ricci, and S. Márka, *Phys. Rev. D* **84**, 082002 (2011), [arXiv:1109.4258 \[gr-qc\]](#).
- [28] M. Pitkin, S. Reid, S. Rowan, and J. Hough, *Living Reviews in Relativity* **14**, 5 (2011), [arXiv:1102.3355 \[astro-ph.IM\]](#).
- [29] S. E. Whitcomb, *Classical and Quantum Gravity* **25**, 114013 (2008).
- [30] D. Sigg and LIGO Science Collaboration, *Classical and Quantum Gravity* **23**, S51 (2006).
- [31] F. Acernese, P. Amico, M. Alshourbagy, F. Antonucci, S. Aoudia, P. Astone, S. Avino, D. Babusci, G. Ballardin, and F. Barone, *Classical and Quantum Gravity* **24**, S381 (2007).
- [32] H. Lück and GEO600 Team, *Classical and Quantum Gravity* **14**, 1471 (1997).
- [33] F. Acernese, M. Agathos, K. Agatsuma, D. Aisa, N. Allemandou, A. Allocca, J. Amarni, P. Astone, G. Balestri, and G. Ballardin, *Classical and Quantum Gravity* **32**, 024001 (2015), [arXiv:1408.3978 \[gr-qc\]](#).
- [34] K. Somiya, *Classical and Quantum Gravity* **29**, 124007 (2012), [arXiv:1111.7185 \[gr-qc\]](#).
- [35] Kagra Collaboration, T. Akutsu, *et al.*, *Nature Astronomy* **3**, 35 (2019).
- [36] C. S. Unnikrishnan, *International Journal of Modern Physics D* **22**, 1341010 (2013), [arXiv:1510.06059 \[physics.ins-det\]](#).
- [37] LIGO and Virgo Collaborations, *Phys. Rev. Lett.* **116**, 061102 (2016).
- [38] The SNR grows with the square root of time. As such for longer observation times, we expect an even more substantial increase in the precision of this measurement. Our model A will generate an SNR of 82 in 5 years and 116 in 10 years. These SNRs correspond to precisions of $\pm 2.4\%$ and $\pm 1.7\%$.